

Spin torque transistor revisited

Takahiro Chiba,^{1, a)} Gerrit E. W. Bauer,^{1, 2, 3} and Saburo Takahashi¹

¹⁾*Institute for Materials Research, Tohoku University, Sendai 980-8577, Japan*

²⁾*WPI-AIMR, Tohoku University, Sendai 980-8577, Japan*

³⁾*Kavli Institute of NanoScience, Delft University of Technology, Lorentzweg 1, 2628 CJ Delft, The Netherlands*

(Dated: 26 September 2018)

We theoretically study the operation of a 4-terminal device consisting of two lateral thin-film spin valves that are coupled by a magnetic insulator such as yttrium iron garnet (YIG) via the spin transfer torque. By magnetoelectronic circuit theory we calculate the current voltage characteristics and find negative differential resistance and differential gain in a large region of parameter space. We demonstrate that functionality is preserved when the control spin valve is replaced by a normal metal film with a large spin Hall angle.

A transistor is a three terminal device that plays important roles in today's electronics. A conventional transistor generates a large current modulation between source and drain terminals by a relatively small signal on the third "base" contact. This property is called "gain" and the corresponding circuit acts as an "amplifier". In the field of spintronics three-terminal devices have been studied since Datta-Das proposed the spin FET,¹ in which the electronic spin degrees of freedom are utilized to achieve new functionalities in circuits and devices made of ferromagnetic and normal conductors. However, with few exceptions^{2,3} spin transistors lack current gain, which is essential for many applications.

A transistor based on the current-induced spin-transfer torque, the so-called spin torque transistor (STT), was proposed a decade ago.³ Figure 1 shows the schematics of the device. The central insulating ferromagnetic disk with in-plane magnetization is sandwiched by normal metal films on both sides that form the spacers of two lateral spin valves (LSVs). The magnetizations in the upper and lower LSVs are parallel to the x and y direction, respectively, forming a closed magnetic flux loop with weak stray fields. An applied voltage V_S drives a current through the lower LSV, generating a spin accumulation in the lower normal metal spacer that exerts a torque on the magnetization of the central magnetic disk in the y -direction. Application of a voltage V_B induces a spin accumulation that creates a spin transfer torque along x , which competes with that of the lower LSV. The magnetization direction of the central layer can therefore be controlled by the relative magnitude of V_S and V_B . The transistor action consists of the control of the source-drain current I_{SD} by the base voltage V_B . This device can display negative differential resistance and gain when the conductance polarization is high and spin-flip scattering is small, even at room temperature.³ Unfortunately, current gain was found only for very

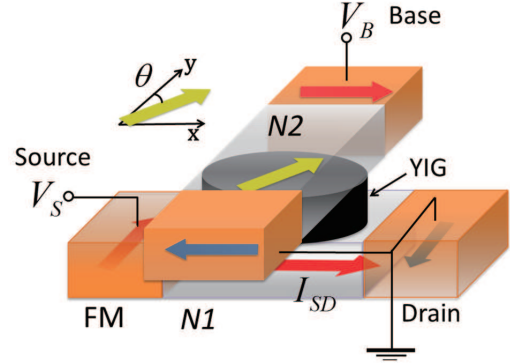


FIG. 1. Schematics of the spin torque transistor.³ The contacts are ferromagnets in a flux closure configuration. The circular disk is made from a magnetic insulator with easy plane magnetization, while the rectangles represent normal metal thin films. θ is the angle between base magnetization and y -axis.

highly polarized magnetic contacts. The originally proposed structure was also complicated, since the central layer was assumed to be a strongly coupled magnetic tunnel junction.

Recently, magnetic insulators have attracted attention as new materials for spintronics. The magnetization of Yttrium iron garnet (YIG), a ferrimagnetic insulator (FI) with a large band gap, can be activated thermally⁴ or electrically⁵ by means of the spin Hall effect (SHE) via a Pt contact and detected electrically in another Pt contact using the inverse SHE (ISHE). Spin transport at a normal metal (N)|FI interface is governed by the spin-mixing conductance $g^{\uparrow\downarrow}$.⁶ The prediction of large $g^{\uparrow\downarrow}$ for interfaces between YIG and simple metals by first-principle calculations⁷ has been confirmed by experiments,⁸ proving that the magnetization in insulators may undergo large spin-transfer torques. We therefore propose here a thin YIG film as central layer of an STT as shown in Fig. 1. Secondly,

^{a)}Electronic mail: t.chiba@imr.tohoku.ac.jp

we suggest to take advantage of the recent discovery of the giant spin Hall effect in Ta⁹ and W¹⁰ or Bi-doped Cu¹¹ to operate the STT, leading to further simplifications of the device design.

The I - V characteristics of the spin torque transistor with a YIG base as shown in Fig. 1 can be computed by magnetoelectronic circuit theory.⁶ We calculate source-drain currents, torques on the base magnetization created by the spin accumulations, and the differential resistance and gain as a function of the voltage ratio V_S/V_B and device parameters.

At the interface between a monodomain ferromagnet with magnetization parallel to the unit vector \mathbf{m} and a paramagnetic metal, the charge and spin currents, I_c and \mathbf{I}_s , driven by charge chemical potential difference $\Delta\mu_c$ and spin accumulation in the normal metal $\Delta\mu_s$ are linear functions of the interface conductances. The conventional conductances $g^{\uparrow\uparrow}$ and $g^{\downarrow\downarrow}$ for electrons with up and down spins, respectively, vanish when the ferromagnet is an insulator. The complex spin-mixing conductance $g^{\uparrow\downarrow}$ governs the spin current polarized transverse to the magnetization. The conductance parameters are in units of the conductance quantum e^2/h , contain (for ferromagnetic metals) bulk and interface contributions, and can be computed from first-principles.¹² For metallic^{12,13} and insulating⁷ ferromagnets, $\text{Im } g^{\uparrow\downarrow}$ is usually smaller than 10% of $\text{Re } g^{\uparrow\downarrow}$ and is disregarded below. It is convenient to introduce $g = g^{\uparrow\uparrow} + g^{\downarrow\downarrow}$ and $p = (g^{\uparrow\uparrow} - g^{\downarrow\downarrow})/g$, where g is the total conductance and p its polarization. The continuity equation for spin current and spin accumulation μ_s^{N1} in N1 reads:

$$\mathbf{I}_s^S + \mathbf{I}_s^D + \mathbf{I}_s^B = \frac{e^2 N(0) V_{ol}}{\tau_{sf}} \mu_s^{N1}, \quad (1)$$

where $\mathbf{I}_s^{S/D/B}$ are the spin currents flowing from the Source/Drain/Base ferromagnets into the spacer N1. $N(0)$ and V_{ol} are the density of states at the Fermi level and the volume, and τ_{sf} is the spin-flip relaxation time. Spin-flip can be disregarded in the normal metal node of small enough structures made from metals with weak spin dissipation such Al,¹⁴ Cu,¹⁵ Ag,¹⁶ or graphene.¹⁷ The spin-flip in the source and drain electrodes can simply be included by taking their magnetically active thickness as the smaller one of the spin-flip diffusion length and physical thickness. The elec-

trically insulating base electrode is assumed to be thin and magnetically soft. The source-drain current I_{SD} has been derived earlier¹⁸ in terms of g_S and p_S , the normal conductance and polarization of the metallic source/drain contacts and $g_S^{\uparrow\downarrow}$ ($g_B^{\uparrow\downarrow}$) is the spin-mixing conductance of the source/drain (insulating base) contacts. I_{SD} depends on the base magnetization angle θ with respect to the y -axis. The torque $\tau_B^{N1}(\theta)$ on the base magnetization created by the spin accumulation in the space is proportional to the transverse spin current into the base.¹⁸ We disregard effects of the Ørsted field produced by I_{SD} . A steady state with finite θ exists when τ_B^{N1} is exactly canceled by an external torque, either from an applied magnetic field or a current-induced torque from the top layer. We assume the same parameters for the upper and lower sections such that $\tau_B^{N2}(\theta)/V_B = \tau_B^{N1}(\pi/2 - \theta)/V_S$ (see Fig. 1), where V_B is the voltage over the upper layer. We keep the ratio between the mixing conductances of metal and insulator variable, *viz.* chose $g_S : g_S^{\uparrow\downarrow} : g_B^{\uparrow\downarrow} = 1 : 1 : \beta$. The stationary state of the biased spin torque transistor is described by the angle θ_0 at which the two torques on the base magnet cancel each other. $\tau_B^{N1}(\theta_0) = \tau_B^{N2}(\theta_0)$ then leads to the transcendental equation

$$\frac{V_S}{V_B} = \frac{\tan^2 \theta_0 + \epsilon}{\epsilon \tan^2 \theta_0 + 1 \tan \theta_0}, \quad (2)$$

where $\epsilon = (\beta + 2)/(2\beta + 2)$. With $\delta = 1/(\beta + 1)$, the source-drain conductance becomes

$$\frac{I_{SD}(V_S, V_B)}{V_S} = \frac{e}{h} \frac{g_S}{2} \left(1 - p_S^2 \frac{\epsilon + \delta \tan^2 \theta_0}{\epsilon + \tan^2 \theta_0} \right). \quad (3)$$

With increasing p_S , strong non-linearities develop that for large polarizations lead to negative differential conductances for $V_S/V_B \gtrsim 1$.

We concentrate on the differential current gain $\Gamma = T/G$ as a representative figure of merit, where $T = (dI_{SD}/dV_B)_{V_S} = (\partial I_{SD}/\partial \theta)_{V_B} (\partial \theta/\partial V_B)_{V_S}$ is the differential transconductance and $G = (dI_{SD}/dV_S)_{V_B} = I_{SD}/V_S + (\partial I_{SD}/\partial \theta)_{V_S} (\partial \theta/\partial V_S)_{V_B}$ the differential source-drain conductance G . While Ref. 3 focused on angles $\theta_0 \rightarrow 0$, we extend the calculations to arbitrary working points θ_0 controlled by the ratio of the applied voltages. The differential gain then reads

$$\Gamma = \frac{2p_S^2(1 - \delta) \tan \theta_0}{1 + (3\epsilon - 1/\epsilon) \tan^2 \theta_0 + \tan^4 \theta_0 - p_S^2 [1 + (3\epsilon - \delta/\epsilon) \tan^2 \theta_0 + \delta \tan^4 \theta_0]}. \quad (4)$$

By substituting the solution of Eq. (2), we calculate the differential current gain Γ as a function of V_S/V_B and plot it in Fig. 2 as a function of the ratio

V_S/V_B and different values of the conductance polarization of the metallic ferromagnetic contacts p_S . The differential current gain can be huge, particularly near

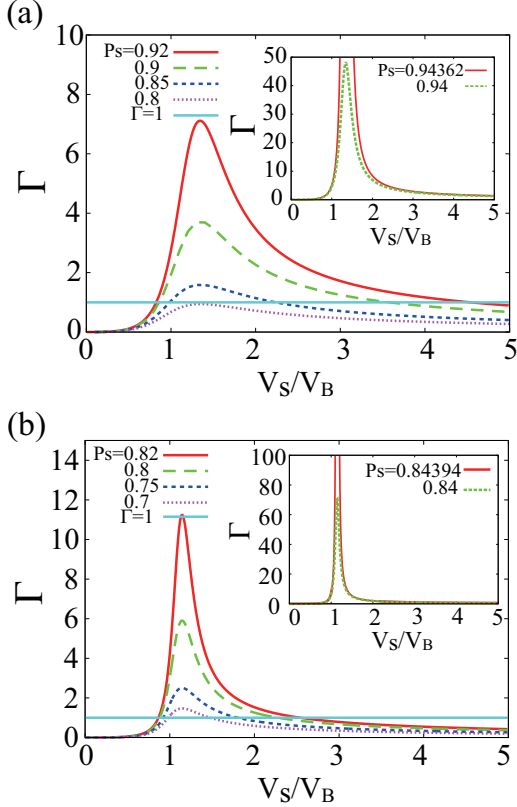


FIG. 2. (a),(b):Differential current gain as a function of the voltage ratio V_S/V_B for different values of p_S (c) $\beta = 1$, (d) $\beta = 5$. Insets represent the infinity gain for the critical value of p_S .

the half-metallic limit of $p_S = 1$, indicating that the contacts should be fabricated from high polarizations materials such as certain Heusler alloys or very thin MgO tunnel junctions. The device performance depends strongly on all parameters and is by no means universal. The critical value of p_S for vanishing differential resistance $G(\theta_0) = 0$ can be computed as

$$p_S(\beta) = \sqrt{\frac{9\epsilon^2 - 1}{9\epsilon^2 - \delta}} = \sqrt{\frac{5\beta^2 + 28\beta + 32}{9\beta^2 + 32\beta + 32}} \quad (5)$$

$$\rightarrow \frac{\sqrt{5}}{3} \simeq 0.74536 \quad (\beta \rightarrow \infty). \quad (6)$$

β can be increased by reducing the source/drain contact areas or by introducing tunnel junctions, although this will increase the response time. It should also be kept in mind that our results are valid only when the spin accumulation is not strongly affected by spin flip assuming that $\mu_s^{N1}/p_S e V_S = 1$. The error involved can be estimated by the spin accumulation of the spin valve for $\theta = 0$, for which the spin accumulation is limited by the spin relaxation according

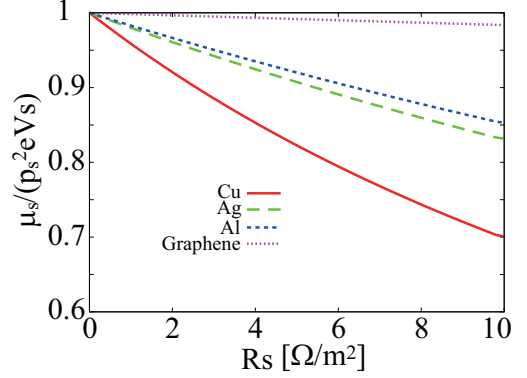


FIG. 3. Spin accumulation in the source-drain spin valve for $\theta = 0$ as a function of the interface resistance $R_S = hA/e^2/g_S$ for a node length of $L_{N1} = 200$ nm.

to¹⁹

$$\frac{\mu_s^{N1}}{p_S^2 e V_S} = \left[1 + \frac{hA}{e^2 g_S} \frac{L_{N1}}{\rho_{N1} \lambda_{N1}^2} \right]^{-1}, \quad (7)$$

where ρ_{N1} is the bulk resistivity, L_{N1} the length, and λ_{N1} the spin diffusion length. Figure 3 shows this ratio for Py|Cu, Py|Ag, Py|Al, Co|Graphene, using the (room temperature) parameters. $\rho_N = 2.9, 2.0, 3.2$ and $3.0 \mu\Omega\text{cm}$, and $\lambda_N = 400, 700, 600$ and 2000 nm for Cu, Ag, Al and Graphene, respectively.^{16,20,21}

The spin Hall effect (SHE)²² refers to the spin current induced transverse to a charge current through a nonmagnetic material with spin-orbit interaction. Recently, large spin Hall effects have been reported in platinum,²³ and CuBi alloy.¹¹ β -tantalum,⁹ and β -tungsten,¹⁰ generate spin Hall currents large enough to induce spin-torque switching of ferromagnetic contacts. The strength of the SHE is measured by the spin Hall angle defined by the ratio, $\alpha_{SH} = I_s/I_c$, where I_s is the transverse spin current induced by a charge current I_c . $\alpha_{SH} = 0.07$ for Pt,²³ -0.15 for β -Ta,⁹ -0.3 for β -W,¹⁰ and -0.24 for CuBi alloy¹¹ have been reported. We therefore suggest the device which we call the spin Hall torque transistor. In the new device, the control spin valve (upper one in Fig. 1) is replaced by a normal metal film with a large spin Hall angle. For the cited values of α_{SH} its performance is comparable to the one discussed above, but easier to fabricate. We point out the interest of simple bilayers of a spin Hall metal and magnetic insulator, in which an new effect has been discovered recently, *viz.* a dependence of the electrical resistance in the normal on the magnetization angle of the neighboring magnetic insulator, the spin Hall magnetoresistance.^{24,25} We can therefore envisage a device in which both spin valves are replaced by films of a metal with a large spin Hall angle. In this case, the steady state

magnetization angle is simply $\theta = \arctan(V_B/V_S)$. However, since the spin Hall magnetoresistance in the lower layer scales like α_{SH}^2 , such a device would be not very attractive unless $\alpha_{\text{SH}} \gtrsim 1$, which has not been reported up to now. We therefore consider in the following a hybrid device consisting of a source-drain lateral spin valve as before, and only replace the upper one by a spin Hall metal.

We treat the upper layer (spin Hall system) by diffusion theory with quantum mechanical boundary conditions at the interface to the insulating magnet.²⁵ At $\theta = 0$ ($\pi/2$) the source-drain current into (or torque on) the magnetic insulator vanishes (is maximal) while that from the upper film is maximal (vanishes). Following Ref. 25, the torque reads:

$$\tau_B^{\text{SH}}(\theta) = \frac{\hbar}{2e} \alpha_{\text{SH}} \frac{A\sigma}{L} V_B \frac{2\lambda G_{B2}^{\uparrow\downarrow} \tanh(d/2\lambda)}{\sigma + 2\lambda G_{B2}^{\uparrow\downarrow} \coth(d/\lambda)} \cos \theta,$$

where d is the film thickness, $A = LW$ the cross section of the contact, with L and W the length and width of the (rectangular) wire in contact with the YIG disk, and $G_{B2}^{\uparrow\downarrow} (= e^2 g_{B2}^{\uparrow\downarrow} / A/h)$ the real part of

the spin-mixing interface conductance per unit area for the top contact.

The torque-induced rotation from $\theta = 0$ suppresses the spin accumulation and increases the source-drain current. As before this may lead to vanishing differential conductance. We choose a model system with p_S and α_{SH} variable, but other parameters fixed, viz. $g_S : g_S^{\uparrow\downarrow} : g_{B1}^{\uparrow\downarrow} : g_{B2}^{\uparrow\downarrow} = 1 : 1 : \beta : \gamma$. The two torques on the base magnet cancel each other, when $\tau_B^{N1}(\theta_0) = \tau_B^{\text{SH}}(\theta_0)$ or

$$F \frac{V_S}{V_B} = \frac{\tan^2 \theta_0 + \epsilon}{\tan^2 \theta_0 + 1} \frac{1}{\tan \theta_0}, \quad (8)$$

where $F \equiv K(1 - \epsilon)$, $\epsilon = (\beta + 2)/(2\beta + 2)$, and

$$K = 2 \frac{e^2 g_S L}{hA} \frac{p_S}{\sigma} \frac{1}{\alpha_{\text{SH}}} \left[\frac{\sigma}{2\gamma\lambda} \frac{hA}{e^2 g_S} + \coth \frac{d}{\lambda} \right] \coth \frac{d}{2\lambda}. \quad (9)$$

The enhancement factor $F \sim L$ scales with the SHE metal wire and the base magnetic insulator contact length because the spin current density is governed by the electric field V_B/L . The differential gain now reads

$$\Gamma = \frac{1}{F} \frac{2p_S^2 \epsilon (1 - \delta) \tan \theta}{\epsilon + (3\epsilon - 1) \tan^2 \theta + \tan^4 \theta - p_S^2 [\epsilon + (3\epsilon - \delta) \tan^2 \theta + \delta \tan^4 \theta]}. \quad (10)$$

By substituting the solution of Eq. (8), we calculate the differential current gain Γ as a function of V_S/V_B and plot it in Fig. 4 for different values of the conductance polarization and the spin Hall angle α_{SH} .

The critical value of p_S at which $G(\theta) = 0$ in Eq. (10) becomes

$$p_S(\beta) = \sqrt{\frac{9\epsilon - 1}{9\epsilon - \delta}} = \sqrt{\frac{7\beta + 16}{9\beta + 16}} \quad (11)$$

$$\rightarrow \frac{\sqrt{7}}{3} \simeq 0.88192 \quad (\beta \rightarrow \infty). \quad (12)$$

The spin (Hall) torque transistors can display negative differential resistance and differential gain by controlling source-drain current by the competing spin transfers on both sides of the base magnetization. We represented the negative differential resistance and gain as a function of the ratio between the base voltage and the source-drain voltage. These device can operate at room temperature, but in order to be useful, ferromagnetic materials with polarizations close to unity and normal metals with a large spin Hall angles are required. These parameters are still quite high, but might be accessible with special materials. The base contact should be a magnetic insulator in order to suppress undesired cross-talk and have a large

mixing conductance with the normal metal, which is known to be the case for YIG.^{7,8} Tunnel junctions or reduced contact areas for the source-drain contacts improve the differential gain but slow down the response time and require reduced spin-flip scattering. The contact between the metals and YIG should be relatively large. Since the current-induced torques due to the spin Hall effect are comparable to that from spin valves, the performance of the spin (Hall) torque transistor can be comparable to the old type, but might be easier to fabricate. We also note that while $p_S \leq 1$, α_{SH} is not limited by any principle.

The spin torque transistors are to our knowledge the only spintronics devices that provide analogue gain; this in contrast to the Oersted field-operated digital scheme in Ref. 2 (that, by the way, could also work with the spin Hall effect). A disadvantage of the spin torque transistor is the stand-by current that is analogous to the leakage current in bipolar transistors. The full electric control of the magnetization direction without need for magnetic field might find applications as well.

This work was supported by FOM (Stichting voor Fundamenteel Onderzoek der Materie), EU-ICT-7 ‘‘MACALO,’’ the ICC-IMR, DFG Priority Programme 1538 ‘‘Spin-Caloric Transport’’ (GO 944/4),

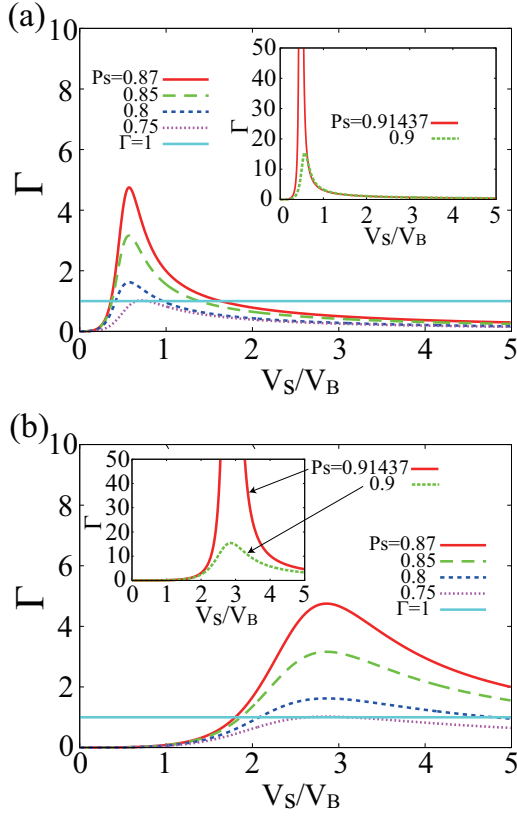


FIG. 4. (a),(b):Differential current gain in the spin (Hall) transistor as a function of the voltage ratio V_S/V_B for different values of p_S and α_{SH} ($\beta = \gamma = 5$, $e^2 g_S/h/(L\sigma) = 1$, $K = 5p_S/6/\alpha_{SH}$) (c) $\alpha_{SH} = 0.3$, (d) $\alpha_{SH} = 1$. Insets represent the infinity gain for the critical value of p_S .

and KAKENHI (No. 22540346).

¹S. Datta and B. Das, Appl. Phys. Lett. **56**, 665 (1990).

²K. Konishi, T. Nozaki, H. Kubota, A. Fukushima, S. Yuasa, and Y. Suzuki, IEEE Trans. Magn. **48**, 1134 (2012).

³G. E. W. Bauer, A. Brataas, Y. Tserkovnyak, and B. J. van Wees, Appl. Phys. Lett. **82**, 3928 (2003).

⁴K. Uchida, J. Xiao, H. Adachi, J. Ohe, S. Takahashi, J. Ieda, T. Ota, Y. Kajiwara, H. Umezawa, H. Kawai, G. E. W. Bauer, S. Maekawa, and E. Saitoh, Nature Mater. **9**, 894 (2010).

⁵Y. Kajiwara, K. Harii, S. Takahashi, J. Ohe, K. Uchida, M. Mizuguchi, H. Umezawa, H. Kawai, K. Ando, K. Takanashi, S. Maekawa, and E. Saitoh, Nature **464**, 262 (2010).

⁶A. Brataas, Yu. V. Nazarov, and G. E. W. Bauer, Phys. Rev. Lett. **84**, 2481 (2000); Eur. Phys. J. B **22**, 99 (2001).

⁷X. Jia, K. Liu, K. Xia, and G. E. W. Bauer, Europhys. Lett. **96**, 17005 (2011).

⁸C. Burrowes, B. Heinrich, B. Kardasz, E. A. Montoya, E. Girt, Y. Sun, Y. Y. Song, and M. Wu, Appl. Phys. Lett. **100**, 092403 (2012).

⁹L. Liu, C.-F. Pai, Y. Li, H. W. Tseng, D. C. Ralph, R. A. Buhrman, Science **336**, 555 (2012).

¹⁰C.-F. Pai, L. Liu, Y. Li, H. W. Tseng, D. C. Ralph, and R. A. Buhrman, Appl. Phys. Lett. **101**, 122404 (2012).

¹¹Y. Niimi, Y. Kawanishi, D. H. Weil, C. Deranlot, H. X. Yang, M. Chshiev, T. Valet, A. Fert, and Y. Otani, Phys. Rev. Lett. **109**, 156602 (2012).

¹²K. Xia, P. J. Kelly, G. E. W. Bauer, A. Brataas, and I. Turek, Phys. Rev. B **65**, 220401 (2002).

¹³M. D. Stiles and A. Zangwill, Phys. Rev. B **66**, 14407 (2002).

¹⁴F. J. Jedema, H. B. Heersche, A. T. Filip, J. J. A. Baselmans, and B. J. van Wees, ibid. **416**, 713 (2002); S. O. Valenzuela and M. Tinkham, Nature **442**, 176 (2006).

¹⁵F. J. Jedema, A. T. Filip, and B. J. van Wees, Nature (London) **410**, 345 (2000).

¹⁶T. Kimura and Y. Otani, Phys. Rev. Lett. **99**, 196604 (2007).

¹⁷M. Wojtaszek, I. J. Vera-Marun, T. Maassen, and B. J. van Wees, Phys. Rev. B **87**, 081402(R) (2013).

¹⁸G. E. W. Bauer, Y. Tserkovnyak, D. Huertas, and A. Brataas, Phys. Rev. B **67**, 094421 (2003).

¹⁹A. Brataas, Y. V. Nazarov, J. Inoue, G. E. W. Bauer, Phys. Rev. B **59**, 93 (1999); Eur. Phys. J. B **9**, 421 (1999).

²⁰F. J. Jedema, M. S. Nijboer, A. T. Filip, and B. J. van Wees, Phys. Rev. B **67**, 085319 (2003); J. Bass and W. P. Pratt, J. Phys. Condens. Matter **19**, 183201 (2007).

²¹W. Han and R. K. Kawakami, Phys. Rev. Lett. **107**, 047207 (2011); M. H. D. Guimarães, A. Veligura, P. J. Zomer, T. Maassen, I. J. Vera-Marun, N. Tombros, and B. J. van Wees, Nano Lett. **12**, 3512 (2012).

²²M. I. Dyakonov and V. I. Perel, Phys. Lett. A **35**, 459 (1971); J. E. Hirsch, Phys. Rev. Lett. **83**, 1834 (1999); S. F. Zhang, Phys. Rev. Lett. **85**, 393 (2000).

²³T. Kimura, Y. Otani, T. Sato, S. Takahashi, and S. Maekawa, Phys. Rev. Lett. **98**, 156601 (2007); K. Ando, S. Takahashi, K. Harii, K. Sasage, J. Ieda, S. Maekawa, and E. Saitoh, Phys. Rev. Lett. **101**, 036601 (2008); O. Mosendz, J. E. Pearson, F. Y. Fradin, G. E. W. Bauer, S. D. Bader, and A. Hoffmann, Phys. Rev. Lett. **104**, 046601 (2010); L. Q. Liu, T. Moriyama, D. C. Ralph, and R. A. Buhrman, Phys. Rev. Lett. **106**, 036601 (2011); L. Q. Liu, O. J. Lee, T. D. Gudmundsen, R. A. Buhrman, and D. C. Ralph, arXiv:1110.6846; L. Q. Liu, R. A. Buhrman, and D. C. Ralph, arXiv:1111.3702.

²⁴H. Nakayama, M. Althammer, Y.-T. Chen, K. Uchida, Y. Kajiwara, D. Kikuchi, T. Ohtani, S. Geprägs, M. Opel, S. Takahashi, R. Gross, G. E. W. Bauer, S. T. B. Goennenwein, E. Saitoh, arXiv:1211.0098.

²⁵Y. Chen, S. Takahashi, H. Nakayama, M. Althammer, S. T. B. Goennenwein, E. Saitoh, G. E. W. Bauer, arXiv:1302.1352.